International Journal of Advanced Technology and Engineering Exploration, Vol 11(121)
ISSN (Print): 2394-5443 ISSN (Online): 2394-7454
http://dx.doi.org/10.19101/IJATEE.2023.10102317

Research Article

Robust facial recognition using deep learning and modified whale optimization algorithm for biometric authentication

M. Leelavathi[1, 2*] and D. Kannan[3]
Research scholar, Department of Computer Science, Pollachi College of Arts and Science, Coimbatore, Tamil Nadu, India[1]
Assistant Professor, Department of AI&ML, Sree Saraswathi Thyagaraja College, Pollachi, Coimbatore, Tamil Nadu, India[2]
Professor, Department of Computer Science, Pollachi College of Arts and Science, Coimbatore, Tamil Nadu, India[3]

Received: 21-September-2023; Revised: 15-December-2024; Accepted: 17-December-2024

Abstract
Face recognition has been a prominent research topic in the field of security. The increasing demand for secure organizational environments and advancements in artificial intelligence has further emphasized the importance of human face recognition. Over time, researchers have explored face recognition methods to accurately identify complete facial images. However, real-world scenarios often involve challenges such as occlusions and noise, which significantly impact recognition accuracy. To address these issues, further development is necessary to enhance performance when dealing with obscured and noisy images. This study presents a simple and efficient deep learning (DL)-based facial recognition method capable of recognizing both occluded and distorted faces. A novel approach, termed robust facial recognition in biometric authentication using the modified whale optimization algorithm (RFRB-MWOA), was introduced. RFRB-MWOA leverages artificial intelligence and advanced DL models to recognize various emotional states effectively. The method employs histogram equalization to standardize brightness and hue levels across different individuals and expressions, ensuring consistent image quality. The process incorporates the mask_convolutional neural network (mask_CNN) model, which uses the modified whale optimization algorithm (MWOA) for hyperparameter tuning. Mask_CNN utilizes probabilistic max-pooling to preserve distinctive features while maintaining feature variability, improving the robustness of the model. Additionally, a layered activation function is applied to produce flexible, normalized information for better generalization. Experimental results demonstrate that the proposed approach outperforms state-of-the-art methods and effectively addresses recognition precision issues caused by input mismatches, showcasing its potential for reliable biometric authentication.

Keywords
Face recognition, Biometric authentication, Deep learning, Mask_convolutional neural network, Whale optimization algorithm.

1.Introduction
The field of biometric systems has undergone significant evolution over the past two decades, driven by advancements in sophisticated digital technologies such as information and communication technology (ICT), the Internet of Things (IoT), the Web of Things (WoT), large-scale memory devices, and high-speed computational processes [1]. Today, biometric-driven safety measures are widely adopted by organizations of all sizes, irrespective of their installation capacity.

*Author for correspondence

Facial recognition plays a critical role in biometric systems, particularly those focused on public security, aiding in the identification of offenders and the prevention of crimes and related activities [2].

The field of computer vision and pattern recognition has also given considerable attention to facial recognition. In light of the global COVID-19 pandemic, there has been a notable shift away from contact-based biometric systems, such as fingerprint recognition, due to health concerns. This transition has led to a surge in interest in facial recognition technologies among biometric vendors [3]. Consequently, many international organizations that previously relied on contact-based biometric technologies have embraced non-touch face identification systems [4]. The increasing demand for non-contact biometric technologies is expected to drive widespread adoption in businesses and influence research institutions to focus on developing advanced systems. Furthermore, it fosters innovation in other biometric technologies, including facial, iris, motion, and voice recognition, paving the way for future advancements in the field [5].

Feature selection and feature extraction techniques play a vital role in the process of face recognition. These techniques can be broadly categorized into global and local approaches [6]. Despite face recognition being a task often associated with global features, local approaches are generally preferred due to their ability to capture finer details and handle variations such as lighting, pose, and occlusion [7].

Numerous studies [8, 9] have explored various local feature extraction techniques that are particularly effective for face recognition. Some prominent methods include local binary pattern (LBP), local ternary pattern (LTP), local derivative pattern (LDP), Weber’s local descriptor (WLB), and histogram of oriented gradients (HOG). These techniques are widely used for their robustness in capturing distinct facial features and improving recognition accuracy in diverse real-world scenarios. Local feature extraction methods are widely regarded as producing superior outcomes compared to global methods in face recognition. This superiority stems from their ability to capture finer, localized details that are crucial for identifying facial features under varying conditions. Recently, the scientific community involved in facial recognition research has shown growing interest in ordinal measurements [10]. Ordinal features, particularly those driven by binarization, have demonstrated resilience against intra-class fluctuations, making them highly effective in handling variations such as lighting, expression, and pose changes. This robustness has positioned ordinal measurements as a promising avenue for improving the accuracy and reliability of facial recognition systems.

According to [11], the measure of ordinal magnitude in biometric technologies indicate the corresponding order of two-colour bands within the particular place or mean intensity of adjacent nearby patches. In depicting and identifying facial images, colour feature is significant. As a result of recent developments in machine learning (ML), deep learning (DL), the availability of high-end hardware, and the abundance of data, various methods for face recognition have been developed that perform exceptionally well [12]. Due to recent developments, computerized facial recognition tools are now used in various real-world situations, from social network photo tagging and photo organization to vital criminal justice uses like searching the missing person and suspected investigations. Identification accuracy is one of the significant parameters to gauge a face recognition model's efficiency [13]. Additionally, its resilience concerning the various data variances requires assessment.

The challenges associated with automated face recognition remain significant, as it is a more recent research focus compared to technologies like fingerprint recognition. For example, Zhang et al. [14] highlighted the issue of facial feature detection, a critical area for the advancement of this technology. Most face detection methods are computationally intensive and often result in suboptimal recognition accuracy. Factors such as gender, age, positional variations, lighting normalization, and opacity have been examined in facial identification studies [15].

Recognizing faces accurately in unrestricted contexts is particularly challenging due to a significant drop in identification accuracy under such conditions. This indicates the need for methods that can enhance facial recognition performance in these scenarios. Tu et al. [16] attempted to address challenges related to illumination and pose by employing deep learning networks and neural network techniques, presenting a promising approach to improve face recognition accuracy.

However, this method has struggled to effectively handle large-scale normalized reflectance images and outdoor face identification scenarios. Another significant challenge in face recognition research lies in testing the effectiveness of trial outcomes. The research community has yet to establish consensus on standard datasets for testing. The choice of datasets often depends on the preferences of individual researchers, resulting in a lack of consistency. Moreover, many datasets do not represent real-world scenarios as they are typically created for specific purposes.

Ethnicity poses another challenge, as there is no reasonably balanced dataset that adequately accounts for factors such as skin color, gender, and age. Additionally, varying lighting conditions at different angles introduce the issue of uneven illumination, causing inconsistencies in the amount of light reflected by the face. This inconsistency can lead to incorrect identification [17]. Similarly, random movement caused by individual motion can result in misclassification during four-dimensional recognition. The rotation of an image can also cause the input image and reference image to appear different, further complicating identification [18].

The primary goal of this study is to achieve accurate authentication by incorporating facial expressions. The proposed method improves detection accuracy by utilizing the modified whale optimization algorithm (MWOA) framework in conjunction with mask_convolutional neural network (mask_CNN). Furthermore, the enhanced accuracy demonstrated in this study contributes to increased security and reliability in biometric locks, making it a significant advancement in facial recognition technology.

The increasing importance of security in organizational settings and the growing reliance on artificial intelligence for security purposes indicate the significance of human face recognition. However, real-world challenges such as occlusion and noise significantly affect the accuracy of recognition systems. While the existing methods address obscured and noisy images to some extent, further development is still needed to achieve high accuracy levels.

A low-cost, high-accuracy deep facial recognition technique, mask_CNN, is employed, integrating both feature extraction and decision-making processes. The feature selection process is enhanced through two key improvements. First, recursive chaotic sequences are implemented to improve the quality of the evolving population. Second, a quasi-opposition learning system is developed, leveraging this mechanism to update and refine the positions of agents while retaining the best-performing agents based on their fitness. Additionally, an anti-spoofing mechanism is embedded within the system, utilizing this exact framework to identify faces accurately. The essential linear predictor further strengthens the system with its high accuracy and ease of learning.

This study introduces a novel and efficient DL-based facial recognition method capable of accurately identifying occluded and distorted faces. The proposed robust facial recognition in biometric authentication using the modified whale optimization algorithm (RFRB-MWOA) utilizes artificial intelligence and advanced DL models to recognize varied emotional states effectively. The approach incorporates histogram equalization to standardize image brightness and hue levels and employs the mask_CNN model optimized with the MWOA algorithm for hyperparameter tuning. To address feature inconsistencies, mask_CNN integrates probabilistic max-pooling, retaining distinctive features while preserving variability. Additionally, the application of layered activation functions enhances the flexibility and efficiency of information normalization, ensuring robust and accurate facial recognition.

The organization of the paper is as follows: Section 2 reviews the previous investigations, section 3 outlines the proposed approach and techniques, section 4 presents the experimental findings, section 5 offers a discussion, and section 6 concludes with the summary and potential directions for future research.

2.Related works

In recent years, researchers had increasingly focused on DL approaches due to their high automatic detection capabilities, despite the significant efficacy achieved by conventional facial recognition methods using handcrafted feature extraction. In this context, some of the most recent research in facial recognition had been discussed, highlighting the methods for deep neural networks (DNN) and feature selection using optimization techniques that enhances recognition performance.

Luque et al. [19] Presented the end-to-end architecture for biometric identification via the convolutional networks utilizing biosensors. The validation strategy, which used convolutional network-based algorithms and actual signals, seemed feasible in the existing surveillance processes in e-health and exercise settings, demonstrating the outstanding promise as biometry. In Donuk et al. [20], feature matrix in the linked CNN layer developed during the second phase was subjected to the binary particle swarm optimization (BPSO) method for selecting features. A support vector machine (SVM) is used to categorize particular characteristics. Lokku et al. [21] created the optimal face recognition network (OPFaceNet) to identify faces with significant noise and occlusion in photos. The noise-specific feature patterns, such as LBP, fuzzy local binary pattern (FLBP), and noise-resistant local binary pattern (NRLBP), were extracted. The suggested CNN classifier utilized the average of three patterns. The fitness sorted rider optimization algorithm (FS-ROA) optimization was the primary contribution that improves the CNN model. Sahan et al. [22] introduced a new face identification method combining a new one-dimensional CNN, CNN deep classifiers with linear discriminative analysis techniques. Bidirectional long short-term memory (BiLSTM)-CNN model was suggested in Febrian et al. [23], along with trials on the CK+ dataset and the assessment of created models' accuracy rate. The dataset was enhanced with additional data to enhance model performance and avoid overfitting. Hu et al. [24] described the creation of an approach for utilizing CNN in biometric identification, based on the user face geometry assessment. It was proposed that the approach for adapting the structural characteristics of CNN to the predicted surrounding in system used the developed biometric authentication. It was suggested that the architectural parameters of CNN had been adjusted in accordance with the resembling typical user recognition of facial images, considered the unique aspects of machine input and presentation. In Page et al. [25], it demonstrated a low-power, integrated electrocardiogram (ECG)—pattern detection system for biometric identification. As the acceptance of devices grows, it is anticipated that ECG combined with the secondary biometric marker such as a fingerprint, played an essential role in wearing protection. The primary goal of this study was to construct the dependable, resilient, and speedy system with restricted surface and energy impact. Benradi et al. [26] presented an innovative approach that utilized the extracted features with HOG and scale-invariant feature transformed (SIFT) to improve face recognition performance despite variability and obstruction. Using the methodologies above, they performed the feature extraction operation before passing the results to CNN architecture. Our simulations' findings demonstrated the SIFT+CNN combination's strong performance. The hybrid ensemble convolutional neural network (HE-CNN) framework for face recognition was proposed in Anwarul et al. [27], used ensemble transfer learning from the altered pre-trained models. The model that considerably increased recognition accuracy was trained using progressive training. Revathy et al. [28] proposed an electronic voting system using face recognition and DL. To finish the selection procedure, the blind verification method and the application of blockchain technology were utilized Wen [29].

After examining the methods above, it was concluded that some needed more computing time, were more complex, and had worse accuracy. Mask_CNN was introduced with the modified optimization method optimizing the fusion process to achieve improved accuracy Abd and Mirjalili [30]. One research gap lies in the need for greater efficiency and accuracy in facial recognition methods amidst the prevalence of DL approaches. While the recent research had focused on DNN and feature selection using optimization techniques, some methods faced the challenges such as increased computational demands and lowered accuracy. Specifically, there was the need for approaches that balanced accuracy, efficiency, and complexity Rahnamayan et al. [31]. Additionally, existing methods often struggled with facial image noise, occlusion, and variability. This highlighted the need for novel approaches that addressed these challenges while maintaining the high levels of accuracy and efficiency [32]. Introduction of mask_CNN with a modified optimization method bridged this gap by improving accuracy through a fusion process.

Recent research in facial recognition had explored the various methods that utilized DL and optimization techniques. One approach, utilizing convolutional networks with biosensors, showed promise for biometric identification in e-health and exercise settings Jain and Learned-miller [33]. Another method used BPSO for feature selection to enhance the classification accuracy using SVM. Optimal face recognition network (OPFaceNet) addressed the noise and occlusion challenges, utilizing a novel CNN classifier optimized by FS-ROA Sonon et al. [34]. BiLSTM-CNN and HOG-SIFT feature extraction improved recognition accuracy, albeit with varying computational complexity. HE-CNN utilized ensemble transfer learning, enhanced the accuracy through progressive training Vadim et al. [35]. However, challenges persisted including the longer computing times and reduced accuracy in certain methods. The proposed mask_CNN with modified optimization aimed to mitigate these challenges, offering improved accuracy through fusion. However, further research was needed to balance accuracy, efficiency, and complexity while addressing noise and variability in facial images Guleria et al. [36].

The reviewed works highlight advancements in facial recognition through DL and optimization techniques, including the application of convolutional networks with biosensors for biometric identification in specific settings.Other studies introduced optimization methods, such as BPSO and FS-ROA, and innovative architectures like BiLSTM-CNN and HE-CNN, addressing challenges of noise and occlusion. However, issues like high computational demands, reduced accuracy, and dataset variability persisted. The introduction of mask_CNN with a modified optimization method bridged these gaps by improving accuracy and efficiency, although further research is needed to balance these aspects while addressing real-world challenges.

3.Materials and methods

System model

Face recognition using amask_CNN system with decision-level fusion is divided into three phases: CNN-based feature extraction, feature selection using MWOA, and decision-level fusion. The entire process of the proposed technique is depicted in *Figure 1*. The proposed method begins with pre-processing the input image. Mask_CNN system undergoes training on the face detection dataset WIDER FACE dataset and benchmark face detection dataset and benchmark (FDDB) sample to extract the relevant features for face recognition. The Mahalanobis separation and the Euclidean distance are utilized to determine the resemblance of the vector's characteristics to merge.

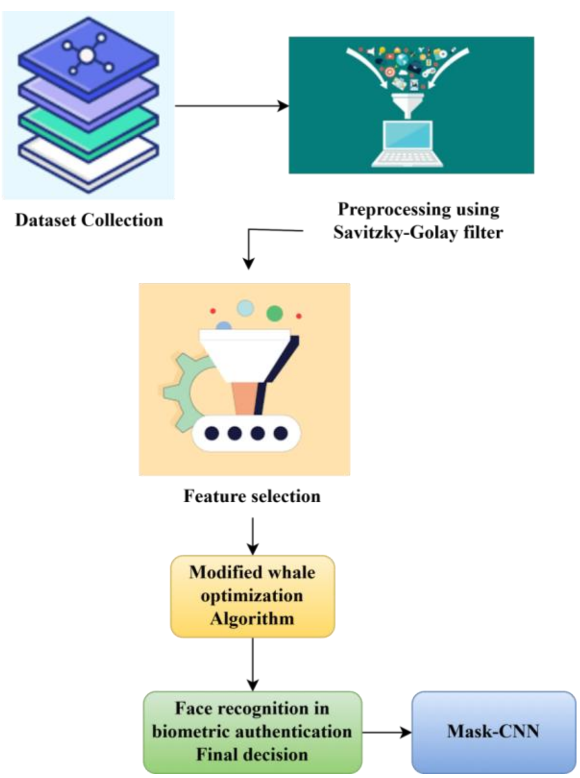

Figure 1 Block diagram for facial recognition in biometric authentication

MWOA selects the features by iteratively optimizing feature subsets, mimicking natural whale behaviour. Candidates represent the different feature combinations evaluated by fitness function. MWOA balances exploration and exploitation phases, where the individuals explore new regions and exploit promising ones. Effectiveness of the feature sets is assessed based on the classification performance metrics such as accuracy, precision, and recall. Additionally, dimensionality reduction, generalization to unseen data, computational efficiency, and robustness to noise are considered. MWOA aims to identify the optimal feature subsets contributing significantly in the task, ensuring efficient and effective feature selection in various applications.

Mask_CNN architecture comprises of convolutional, pooling, normalization, and fully connected layers for effective feature extraction and classification. Convolutional layers capture spatial patterns, followed by pooling layers for spatial dimension reduction. Normalization layers stabilize training, and fully connected layers map features to the output classes. Configurations like filter numbers and layer sizes are tailored to task complexity. During the training, loss function quantifies prediction disparities and is optimized through the algorithms like stochastic gradient descent or Adam. Batch size determines the simultaneous sample processing, while the number of epochs controls dataset iterations. Regularization techniques mitigate overfitting, ensuring robust model performance in mask_CNN system.

The criteria for decision-level fusion in mask_CNN system encompass several vital factors. These include the confidence scores generated by individual CNN models for each input image, the consistency of predictions across multiple models, and the diversity of features captured by each model. Additionally, criteria such as the reliability of each model, their respective accuracies, and any available contextual information influence the decision-level fusion process. A weighted combination or voting mechanism is utilized, where the models with higher confidence scores or accuracies contribute more significantly to the final decision.

3.1Preprocessing of images

Initially, the Savitzky-Golay filter is used to process the pictures from FDDB and WIDERFACE dataset. The primary benefit of this sort of filter is that it reduces distortion while removing noise from a signal, maintain its essential data. Information under consideration is initially fitted using the least square polynomial, and elimination is completed by projecting the input into the signal space. Finally, the polynomial equation is processed using a linear function to retrieve denoised data. Window size for the Savitzky-Golay filter application is typically chosen based on the data's characteristics and the desired smoothing level. Standard window size ranges from 5 to 21 data points, with larger windows providing greater smoothness but potentially blurring the smaller features in signal. It has described the fitting of least square polynomial into data(n) data points. n data points are used to fit the polynomial, Pol(n) in Equation 1.

$$Pol(n) = \sum_{p=0}^{N} b_p n^p \quad (1)$$

In which, b_p is the polynomial's p^{th} coefficient. In other words, the goal is to reduce the mean square estimation error as shown in Equation 2.

$$Obj_G = \sum_{n=-W}^{W} (pol(n) - dat(n))^2 \quad (2)$$

An approximate time of "half width" W is included. The zeroth coefficient is provided, as shown in Equation 3.

$$Y_0 = P(0) = b_0 \quad (3)$$

The data is shifted towards, or the source is been modified, the data points are benen examined for $t \neq 0$ concerning $(G+1)$ equations in $(G+1)$ unknown values, the variation of $Obj_G$is obtained and equal to zero. The $(G+1)$ equations in the $(G+1)$ unidentified variables are represented by Equation 4:

$$\sum_{k=0}^{G} (\sum_{n=-W}^{W} n^{(i+p)b_p}) = \sum_{n=-W}^{W} n^i \, d[n] \quad (4)$$

The combination of $(2W+1) \times (G+1)$ are used to express the given equation 4 the formula for this matrix's (n,i) component as shown in Equation 5.

$$mat_{n,i} = n^i - W \leq n \leq W \quad (5)$$

$$where, i = 0,1,2,3 \ldots G$$

The $(G+1) \times (G+1)$ matrix $B$is represented as $A^T A$. The (i,k) element is given as in Equation 6.

$$Wei_{(i,k)} = \sum_{n=-W}^{W} (n)^{i+k} b_k \ldots where\ i,k = 0,1,2, \ldots . G \quad (6)$$

The W information points make up an array called$X$. $E = [E_{-W}, \ldots E_{-1}, E_0, E_1 \ldots E_W]^T$. The adjusted polynomial's assessed variables are presented as $z[z_0, z_1, \ldots z_G]^T$. The required matrix's standard equations are assessed in the Equations; 7, 8 and 9.

$$Zz = A^T A z \quad (7)$$

$$z = (A^T A)^{-1} A^T E \quad (8)$$

$$z = HE \quad (9)$$

The smooth output value,z_0 calculated using the first row of$H$, is the first element in the array$z$. It relies on the input sequence linearly, while H relies on W and G. Therefore, the coefficients discovered for $2W+1$ sample seems to be same. The same values are designated and decided when choosing the subset of data points from the dataset. The ultimate notation for the pre-processed information is $Pre(out)$.

3.2Extraction of raw features

The altered pictures Pre (out) are handled utilizing the 1964 Gabor function, which is the translation distribution of Gaussian function within the frequency domain [29]. Gabor function is applied with the values chosen for frequencies typically ranging from 0.1 to 0.6 cycles per pixel and orientations from 0 to 180 degrees. These parameters are selected to capture the diverse spatial frequency and orientation characteristics in image processing applications.

Gabor function derives the associated features in frequency domain at different scales and paths, and it is the member of windowed Fourier transform family. Additionally, x Gabor function is akin to the biological function of human eye, frequently used for texture identification and produces positive outcomes. The two-dimensional Gabor function is calculated as follows in Equation 10.

$$\emptyset_{\boldsymbol{j}}(x) = k_j^2 exp(-\frac{k_j^2 x^2}{2\sigma^2})(exp(ik_j x) - exp(\frac{\sigma^2}{2}) \quad (10)$$

In this article, 20 frequencies corresponding to 8 locations are selected for alteration, covering the entire frequency domain and providing comprehensive information for potential grouping. As a result, the orientation $u = 0 \sim 7$ and the frequency domain $v = 0 \sim 19$ are equal. In Equation 11, k_j is calculated as shown in the Equations 11 and 12.

$$k_j = \begin{pmatrix} k_{jx} \\ k_{jy} \end{pmatrix} = \begin{pmatrix} k_v \cos \emptyset_u \\ k_v \sin \emptyset_u \end{pmatrix} \quad (11)$$

$$\text{Where, } k_v = 2^{\frac{y+2}{2}\pi}, \emptyset_u = u\frac{\pi}{8} \quad (12)$$

The contour of feature point u matching the distribution $p(u)$ is found using the equation 12. This equation for Gabor function transition, corresponds to the location$u$, is as follows; the characteristic point coordinates of u are(x,y), in Equation 13.

$$\boldsymbol{j_j}(x) = \int p(u') \emptyset_j (u - u') d^2 u' \quad (13)$$

To determine the proper distance between different locations, k-means method, a traditional distance-based approach is used. Distance is used to assess the similarity, with resemblance between two points decreasing as the distance increases, and conversely, closer the points, they show more similarities. Ultimately, each group of items are divided into k clusters. Average value for data objects closes to the k point is computed to promote high-point grouping similarity. Average value of point groups is calculated using Equation 14.

$$\forall_k = \frac{\sum_{i=1}^{n}\{n^i = K\}u_{(i)}}{\sum_{i=1}^{n}\{n^i = K\}} \quad (14)$$

With the centre point of point category, denoted by n^i, is the nearest point group between the data points i and K; where, $i = 1 \ldots n$. Some of the features are thus taken out, including in Equation 15.

$$\forall_k = \{\forall_{k1}, \forall_{k2}, \ldots . \forall_{kn}\} \quad (15)$$

A person's hair, chin, skin, eyebrows, iris, nose, nostrils, ear, forehead, and other facial features are included in this description. $\forall_k$ Subset of these traits are been chosen, which has been accomplished using the MWOA algorithm.

3.3 Histogram equalization of features

Enhancing photographs is the requirement before choosing the characteristics. Thus, histogram equalization is a method that creates a grey map by altering an image's histogram and redistributing all the pixel values to come as near as feasible to the desired histogram that the user specifies. It chooses a transformation function automatically to provide an output image with the consistent histogram. Let $\forall_k S = S(a, b)$ represent an image made up of P distinct grey levels, which are represented by $S = \{S_0, S_1, \ldots S_{P-1}\}$.. The density function of probability $p(S_k)$ for an image S is referred to as in Equation 16.

$$p(S_k) = \frac{n^r}{n} \quad (16)$$

Here n^r is the number of times, the level S_k appears in the input image, and $r = 0,1, \ldots . S - 1$. The total amount of samples in the supplied image is S. The graphical representation of input image is connected to $p(S_k)$, which denotes the number of pixels with the given intensity S_k. The definition of a transformation function fun_s is in Equation 17.

$$fun_s = S_0 + (S_{P-1} - S_0) \quad (17)$$

The histogram equalization's result image is further represented as Y_hist_out(∀_k)=(Y(i,j)). It has shown that irrespective of the input mean, mean luminance of the histogram-equalized images remains in the middle grey level.

3.3.1 Activation of modified whale optimization algorithm (MWOA)

MWOA enhances the original WOA by introducing the several key modifications to improve performance in complex environments. These includes an enhanced exploration strategy that has adapted based on the solution diversity, adaptive search radius adjusts in accordance with the convergence rate of population, and the incorporation of hybrid techniques for local search to refine solutions. Additionally, MWOA uses a dynamic mechanism for tuning the parameters that governs the exploration-exploitation balance, making the algorithm more responsive to changes in the optimization problem. These modifications collectively enable MWOA to effectively address the challenges posed by occluded and distorted facial images in biometric authentication, resulting in higher accuracy and reliability.

A few critical traits have been selected after the recognizing of specific facial regions to achieve accurate results. This section reviews a method that allows significant computational time savings while providing a rough solution to the feature selection problem. To achieve this, MWOA is considered, with *Figure 2* illustrating the selected features from the face.

The two key enhancements are composed of two linked aspects. First, a chaotic sequence based on the tent map enhances quality. This is followed by the introduction of quasi-opposition learning to improve search capabilities in every possible direction. The recursive mapping is chosen initially, and its structure is outlined in Equation 18.

$$R_{t+1} = \begin{cases} \frac{10R_s}{7} R_s < 0.7 \\ \frac{10(1-R_s)}{3} R_s \geq 0.7 \end{cases} \quad (18)$$

When the beginning value $R_1 \in (0,1)$ is chosen at random, Equation 18 is also been used to generate the chaotic sequence of values $\{R_1, R_2, \ldots R_N\}$ with $N - 1$ times. By translating the order of events to solution, the first agent is been created in the following manner, as shown in Equation 19.

$$y_i = y_{i,max} + (y_{i,max} - y_{i,min})R_i \quad (19)$$

The i[th] dimension's topmost edge of y is represented as $y_{i,max}$, whereas the lower barrier is represented as $y_{i,min}$. All of the population's agents map out their starting states in the following Equations 18 and

Equation 20, which results in a chaotic population. After the population is created, opposition learning, essentially a technique for switching from random to symmetric search, significantly enhances the algorithm's search capability. Opposition-based learning appears inflexible and ineffective for adjusting in the narrow time, even though the opposite-learning method substantially improves the algorithm's search power. The proposed quasi-opposite learning method in the research [30,31] introduced randomness to opposition-based learning, resulting in a random location between the initial position and the opposite location, rather than a fixed, uniform location. The formulation for quasi-opposite learning is presented in Equation 20.

$$y^0 = \frac{m+n}{2} + rand\left(\frac{m+n}{2} - y\right) \quad (20)$$

Where in $rand$ is a random number between 0 and 1. Theoretically, the quasi-opposite position has a 50% probability of falling inside the symmetrical point and the centre and a 50% probability of landing beyond the symmetrical point if $rand \in [0, 2]$. Dropping beyond the symmetry point proves more effective for geographical searches, as it enhances convergence speed, whereas dropping within the symmetry point is preferable for algorithm tweaking to improve solution quality. If the variables constituting y are multidimensional, Equation 21, with m and n as vectors, must be applied independently to each dimension of y.

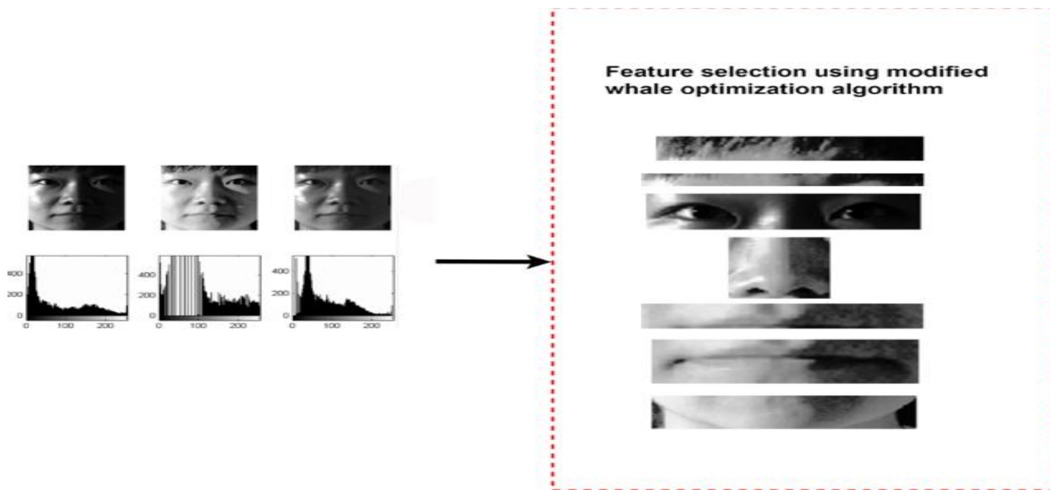

Figure 2 Feature selection using optimization method

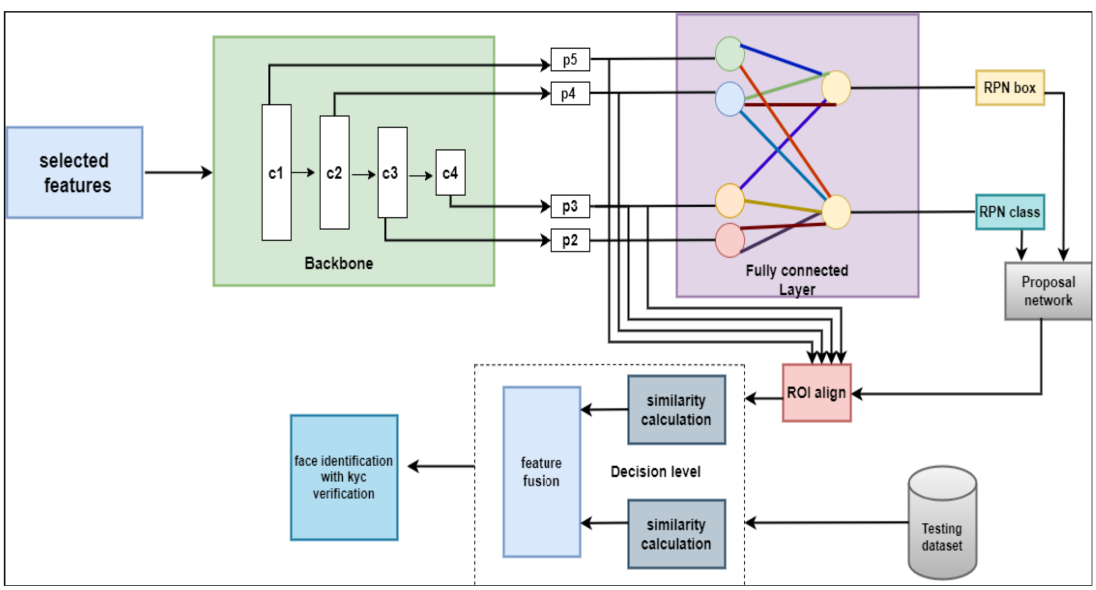

Figure 3 Architecture of mask_CNN

$$y^{0\prime} = \frac{m'+n'}{2} + rand(\frac{m'+n'}{2} - y') \quad (21)$$

As a result, as previously stated, opposition-based learning and Chaotic processes are applied to enhance the geographical search capabilities.

The MWOA employs a combination of chaotic sequences and opposition-based learning to select facial features efficiently. Initially, chaotic sequences generated using a tent map help diversify the search space. Then, opposition-based learning enhances search capabilities by transitioning from random to symmetric search. Quasi-opposite learning further improves the algorithm's effectiveness by introducing randomness, promoting convergence speed, and enhancing solution quality. Features are evaluated based on their ability to represent vital facial regions accurately, such as hair, chin, skin, etc. The algorithm selects features by iteratively optimizing feature sets that best capture facial characteristics. Evaluation criteria include feature relevance, discriminative power, and computational efficiency. By balancing these factors, the MWOA aims to select a subset of features that maximizes recognition accuracy while minimizing computational complexity.

3.4Mask_CNN-based decision

The normalization layer, activation function layer, and decision layer constitute the mask_CNN model proposed in this study. The Softmax classifier, a predictor for facial traits in this technique, is removed after CNN has been pre-trained using a large sample set.

Data normalization: To avoid overfitting and ensure effective gradient descent, selecting a minimal learning rate during network pre-training is typically crucial. Data is normalized across all dimensions to address this issue and ensure they follow the same distribution. When utilizing a high learning rate, normalization can prevent overfitting. Assuming a layer's output has dimensions,$q = \{q^{(1)}, q^{(2)}, .. q^{(\beta)}\}$, the normalization was applied separately to each dimension. Then, for purposes of explanation, for instance, consider every aspect wherein the data of a mini-batch sample with the size of can be defined as $mini_q = q_1, q_2, \dots q_s$. The normalized sample data is $mini_y = y_1, y_2, \dots y_s, y_i (i \in [1, samp])$ and follows the conventional normal distribution with a mean of 0 and a variance of 1. Considering the outcome of the loss function, the sum of the factors can be calculated. $Loss_{fn}$ the combination coefficient $\propto$ and ε depiction is shown in Equations 22 and 23.

$$\frac{\partial Loss\_fn}{\partial \propto} = \frac{\partial Loss\_fn}{\partial \mu_B}\frac{\partial \mu_B}{\partial \alpha} = \frac{\partial Loss_{fn}}{\partial \mu_B}(\mu - \mu_B) \quad (22)$$

$$\frac{\partial Loss\_fn}{\partial \varepsilon} = \frac{\partial Loss\_fn}{\partial (\sigma_b^2)}\frac{\partial (\sigma_b^2)}{\partial \propto} = \frac{\partial Loss_{fn}}{\partial (\sigma_b^2)}(\sigma^2 - \sigma_B^2) \quad (23)$$

Because normalization in the mini-batch was more successful than in all aspects due to the synchronization of the estimation, the information was normalized using the mini-batch to achieve an identical distribution. Additionally, it would be great if the mean and variance were unique to each dimension, but this wasn't feasible. The standard deviation and mean of every dimension have been identified employing the mini-batch data's median and variance to make the normalized computation process easier. All and some of these values were then linked by revising the entire variation and standard. The overall architecture for mask_CNN is shown in *Figure 3*.

Layer of the activation function: The activating procedure introduces nonlinearity into the mask_CNN network. Researchers propose a layered activating operation to address three key issues: providing adaptivity to the activation function, enhancing the non-linear expression capability, and resolving gradient saturation and diffusion problems. The third figure illustrates a three-level architecture with minimal components and learnable activation features. In this binary tree structure, each middle-level node represents the combined output of two lower-level nodes, while the high-level node corresponds to the overall output. Then, $q(in)$ represents the normalized input parameter, while fun_{low}, fun_{mid} and fun_{high}, denote low-, middle-, and high-level node operations. The three-level node function is documented in Equation 24.

$$fun(q(in)) = (\begin{cases} fun_{low}^{n}(q(in)) & low \\ \sigma(\omega q(in)) fun_{mid}^{k,left}(q(in)) + \\ \max\limits_{1\le k\le t} fun_{mid}^{k}(q(in)) \ high \end{cases}$$

$$(1 - \sigma(\omega q(in)) fun_{mid}^{k,right}(q(in)), mid \quad (24)$$

Where, $fun_{low}^{n}(.)$is represents the n-th low-level node function $(fun_{relu}(.) of fun_{elu}(.)), \sigma(.)$is sigmoid function, $fun_{mid}^{k,left}(.)$ and $fun_{mid}^{k,right}(.)$represent the left or right node children functionalities of the k−th middle node correspondingly. The fundamental mechanism for activation is provided using Equations 25 and 26.

$$fun_{relu}(q(in)) = \begin{cases} q(in), & q(in) > 0 \\ w1q(in), & q(in) \le 0 \end{cases} \quad (25)$$

$$fun_{elu}(q(in)) = \begin{cases} q(in), & q(in) > 0 \\ w2(e^{q(in)} - 1) & q(in) \leq 0 \end{cases} \quad (26)$$

The weights of the negative portion of control, known as $w1$ and $w2$, are learned from data and are used in the calculation. The initial values of $w1$ and $w2$ are 0.50 and 1, respectively. The middle-node function fun_{mid}^{k} is represented by Equations 27 and 28.

$$fun_{mid}(q(in)) = \sigma(\omega q(in)) fun_{relu}(q(in)) + (1 - \sigma(\omega q(in)) fun_{elu}(q(in)) \quad (27)$$

$$fun(feature) = fun_{low}, fun_{mid} + fun_{high} \; (28)$$

The maximum of t middle-node functions is the high-level node function, fun_{high}.The two primary activated functions' benefits were as follows: The linear element of the fun_elumakes it achievable to minimize gradient dissolution, and the soft-saturation can decrease the incline from predetermined or fixed limits to zero, which may speed up model learning. The fun_{relu}allows the gradient of the negative value to be extracted from the data, improving the computation that the activation function can learn.

Assuming $fun(feature)$ is a blend of all the features chosen for the mask_CNN feature; it comprises two trained eigenvectors, eig'_1 and eig'_2 , for the set of images and query face pictures, accordingly. The formula that follows is used to determine the resemblance sim^{mask_CNN} eigenvector in Equation 29.

$$sim^{mask\_CNN} = \frac{(eig'_1)^T . eig'_2}{|eig'_1| \times |eig'_2|} \quad (29)$$

where T is the transposition and $|\cdot|$ is the normalization factor. The similarity among gallery face picture gal_i and query facial picture que_i is determined using the resemblance of the attributes obtained in Equation 30.

$$dist(gal_i que_i) = \sum_{k=1}^{dist} \left\| eig'^{(i)}_{1(k)} - eig'^{(j)}_{1(k)} \right\|^2 \; (30)$$

In which $\sum_{k=1}^{dist} \left\| eig'^{(i)}_{1(k)} - eig'^{(j)}_{1(k)} \right\|^2$ indicate the geometric separation between two eigenvectors. The subsequent calculation determines decision-level convergence in Equation 31.

$$dec_{conv} = \varphi dec^{mask\_CNN} + (1 - \varphi) dec^{mask\_CNN} \quad (31)$$

Defined amongst them as the degree of similarity (φ<1)is the fusing similarity, and $dec^{mask_CNN}$is the normalized resemblance of colour mask_CNN.

The mask_CNN architecture comprises several layers: normalization, activation function, and decision. The normalization layer ensures data consistency by normalizing across all dimensions, mitigating overfitting and ensuring effective gradient descent during pre-training. The activation function layer adds nonlinearity and adaptivity to the network, resolving gradient saturation and diffusion issues. It employs three-level architecture with minimal components linked by learnable activation features, utilizing functions like rectified linear unit (ReLU) and exponential linear unit (ELU) to introduce nonlinearity and control gradient behaviour.

The training process for mask_CNN involves selecting a subset of facial features represented as eigenvectors. These eigenvectors capture key facial characteristics and are used to calculate the similarity between gallery and query facial images. The training involves determining the resemblance of these eigenvectors and computing decision-level convergence based on similarity fusion. The loss function, optimization algorithm, batch size, and number of epochs used in training are yet to be described. The mask_CNN architecture incorporates normalization, activation, and decision layers. Details on the optimization algorithm, batch size, epochs, and loss function are necessary for training.

3.5Know your customer (KYC) verification

The KYC verification procedure begins following the evaluation of facial features. A person's live feed is captured, and their face is successfully identified using the trust value reported in the upper right corner. Although it is evident that someone is attempting to trick our system by using a staged photo of the same person, the level of trust decreases dramatically and the fraudulent activity is successfully stopped by a caution message. The trust level in KYC verification is determined by facial recognition accuracy, liveness detection, biometric match confidence, consistency checks, contextual analysis, and fraud detection algorithms, with predefined thresholds for validation.

RFRB-MWOA benefits from the parallel processing capabilities of CNNs, allowing for faster inference times than traditional methods. By efficiently utilizing hardware resources such as graphics processing unit (GPU)s, RFRB-MWOA can process images rapidly, enabling real-time or near-real-time performance in facial recognition tasks. Additionally, the optimization techniques employed in RFRB-

MWOA, such as the proposed RFRB-MWOA, further enhance computational efficiency by reducing redundancy and improving model convergence. The method demonstrates resilience to lighting variations, maintaining reliable detection across different illumination levels. Moreover, it effectively detects faces across various facial orientations, including frontal, profile, and tilted angles. Additionally, the method shows promising results in recognizing facial expressions accurately and identifying subtle variations in emotions. Overall, these findings indicate the versatility and efficacy of the RFRB-MWOA method in addressing challenges posed by diverse environmental conditions and facial characteristics in facial recognition tasks.

4. Results

The studies were conducted using the Ubuntu 16.04 OS, an NVIDIA GEFORCE GTX 1060 GPU, 16 GB of RAM, an Intel i7-7700 CPU, the Python 3.5 software platform, and TensorFlow 1.2.1, as the interface program on a cross-platform desktop machine. Accuracy, precision, recall, and F-score were selected as the metrics for evaluation.

4.1Dataset

The WIDER FACE dataset is a widely used collection for facial detection, known for its extensive diversity in size, posture, and lighting conditions. In this study, 32,203 images were selected from the dataset, identifying a total of 393,703 facial features. The WIDER FACE dataset is organized into 61 event types, offering a comprehensive range of scenarios for testing facial recognition systems. For each event type, 40% of the data was randomly allocated for training, 10% for validation, and 50% for testing, ensuring a robust evaluation process [32].

Additionally, the FDDB dataset, which includes faces from the labelled faces in the wild (LFW) dataset, was utilized. This dataset comprises 5,171 facial annotations, with image resolutions varying, such as 363×450 and 229×410, providing a diverse set of conditions for assessing facial detection and recognition algorithms [33].

4.2Analysis of modified optimization method for feature selection

Figure 4 and *5* depicts the accuracy evaluation for various optimization methods. When analyzing the FDDB dataset, the existing grey wolf optimization (GWO), graph based particle swarm optimization (GPSO) and FS-ROA achieve 87%, 78% and 75% accuracy. In contrast, the proposed MWOA algorithm achieves an accuracy of 97.9%, outperforming the aforementioned existing methods by 10.9%, 19.9%, and 22.9%. When analyzing the WIDER FACE dataset, the existing methods achieve accuracies of 83%, 80%, and 85%, respectively. In comparison, the proposed MWOA algorithm achieves an accuracy of 99.3%, demonstrating improvements of 16.3%, 19.3%, and 9.3% over these methods. *Figures 6* and *7* depict the analysis of the recognition rate for various similarity measures. When analyzing the FDDB dataset, the cosine method achieves 87.5%, the Euclid method achieves 76%, the Jaccard method achieves 78%, and the Mahal method achieves 98% of the recognition rate. When analyzing the WIDER FACE dataset, the results were 88%, 76.5%, 79%, and 98.6%.

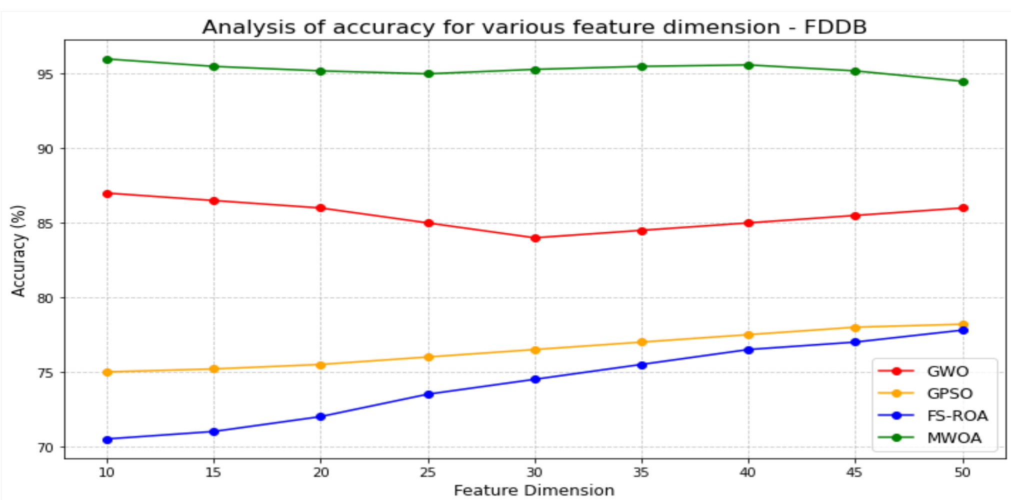

Figure 4 Various feature dimensions with accuracy for the FDDB dataset

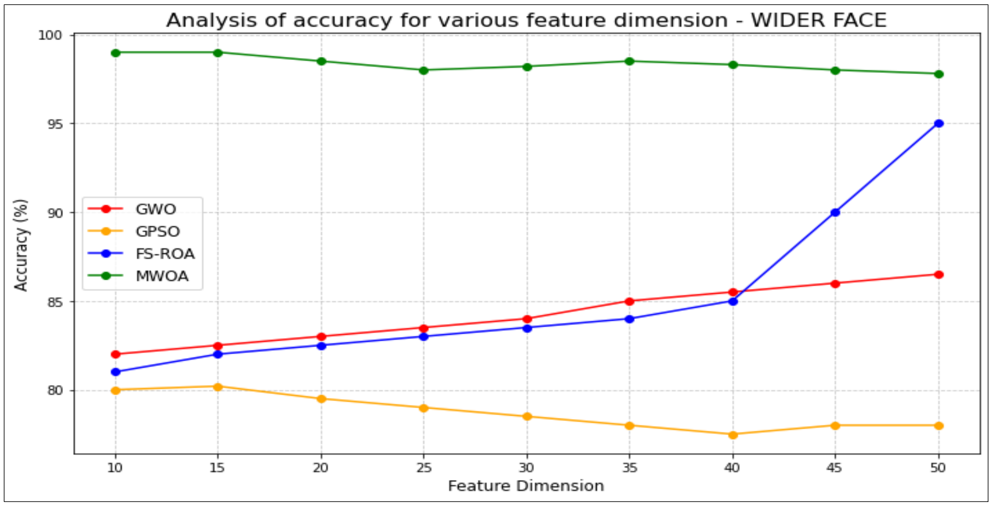

Figure 5 Various feature dimensions with accuracy for the WIDER FACE dataset

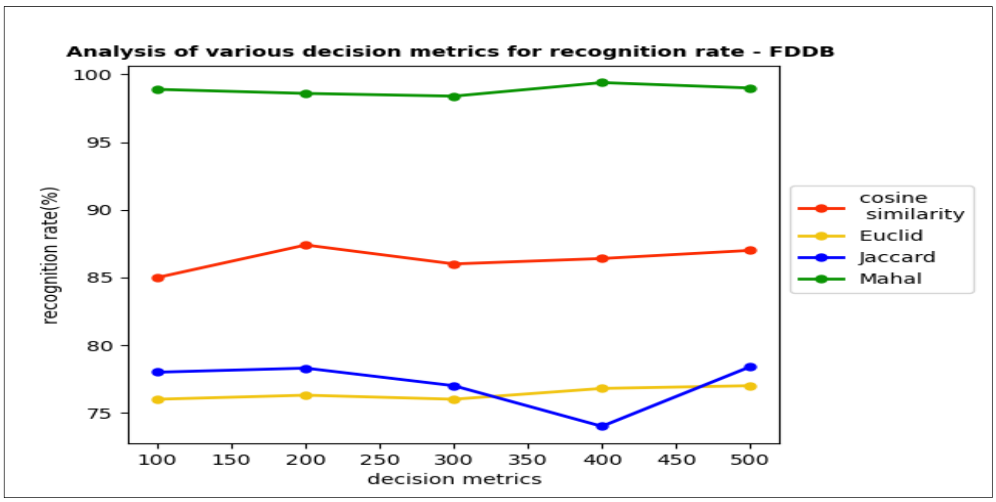

Figure 6 Comparison of recognition rate for the FDDB dataset

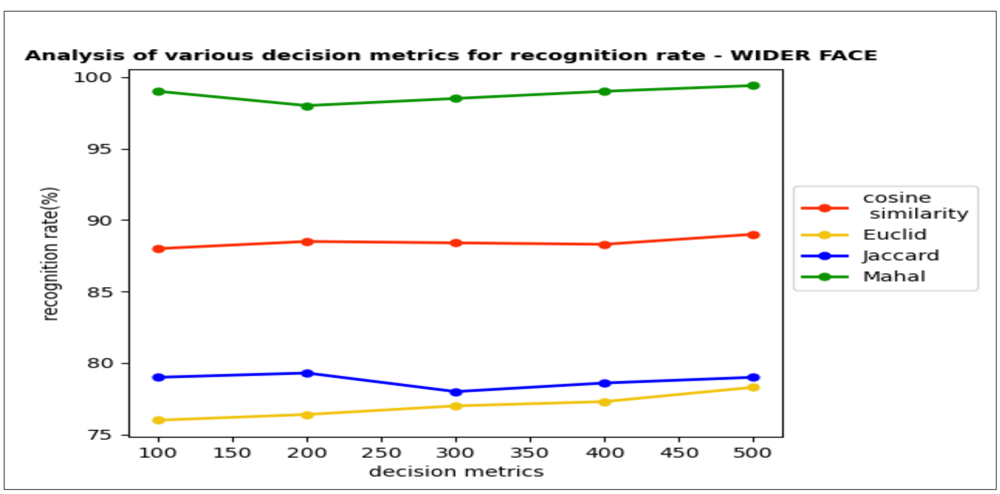

Figure 7 Comparison of recognition rate for the WIDER FACE dataset

4.3Comparison with state-of-the-art methods

Figures 8 and *9* illustrate the precision evaluation between various state-of-the-art methods and the proposed approach. When analyzing the FDDB dataset, the existing methods SIFT+CNN [26], HE-CNN [27], and CNN [21] achieve precision rates of 89%, 72%, and 81%, respectively. In contrast, the proposed RFRB-MWOA achieves a precision of 92%, which is 3%, 20%, and 12% higher than the aforementioned methods. Similarly, when analyzing the WIDER FACE dataset, the existing methods achieve precision rates of 78%, 81%, and 89%, whereas the proposed RFRB-MWOA algorithm achieves 94% precision, demonstrating improvements of 16%, 13%, and 5%, respectively. *Figures 10* and *11* depict the recall evaluation between various state-of-the-art and proposed methods. When analyzing the FDDB dataset, the existing SIFT+CNN [26], HE-CNN [27], and CNN [21] achieves 86%, 75%, and 89% of recall. In contrast, the proposed RFRB-MWOA achieves 93%which is 7%, 18% and 4% better than the aforementioned existing methods; when analyzing the WIDER FACE dataset, we can see that the existing method achieves 79%, 74%, and 82%. In contrast, the proposed RFRB-MWOA algorithm achieves 91% of recall.

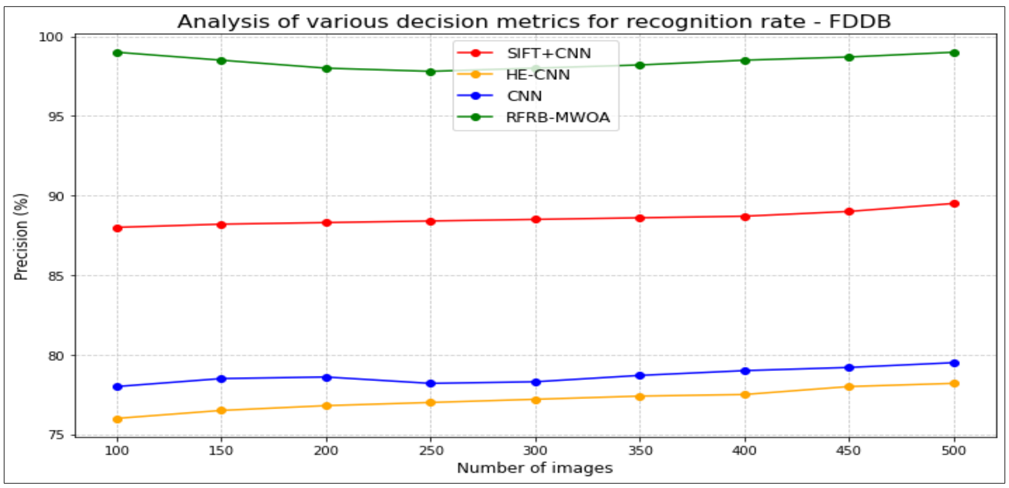

Figure 8 Comparison of precision for the FDDB dataset

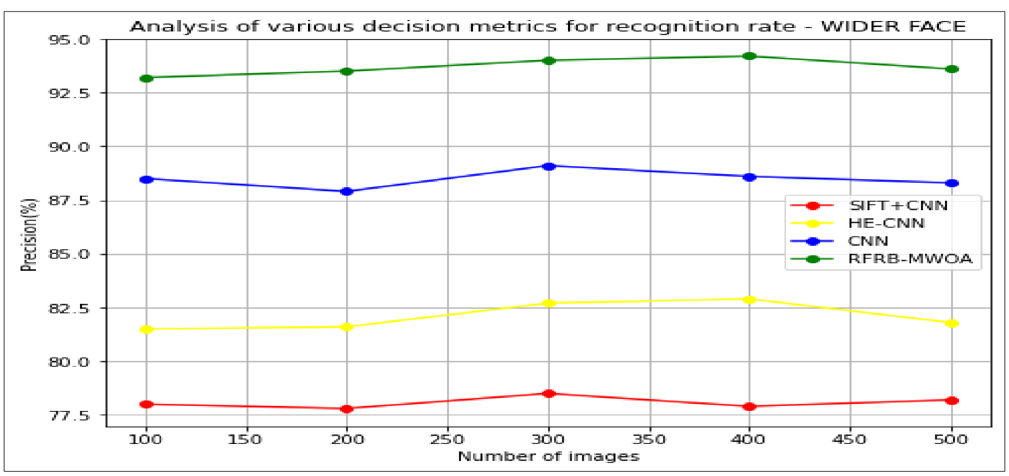

Figure 9 Comparison of precision for the WIDER FACE dataset

Figures 12 and *13* depict the F-score evaluation between various state-of-the-art and proposed methods. When analyzing the FDDB dataset, the existing SIFT+CNN [26], HE-CNN [27], and CNN [21] achieve 72%, 85%, and 87% of F-score. In contrast, the proposed RFRB-MWOA achieves 89%, which is 17%, 4%, and 2% better than the aforementioned existing methods; when analyzing the WIDER FACE dataset, the existing methods achieve 74%, 81%, and 86% F-score, respectively. In contrast, the proposed RFRB-MWOA algorithm achieves 97% of the F-score.

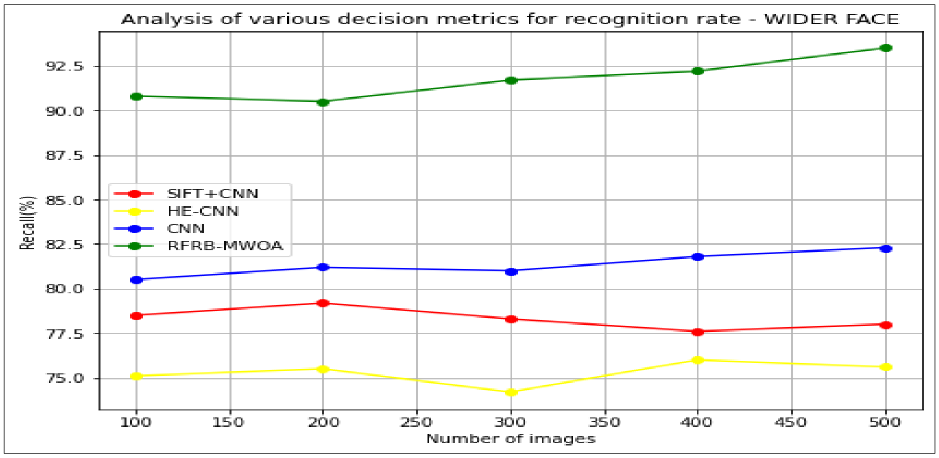

Figure 10 Comparison of recall for FDDB dataset

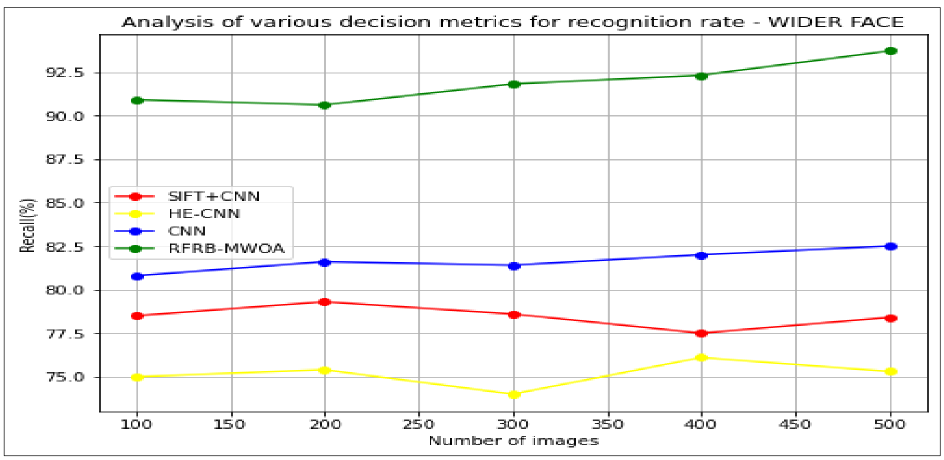

Figure 11 comparison of recall for WIDER FACE dataset

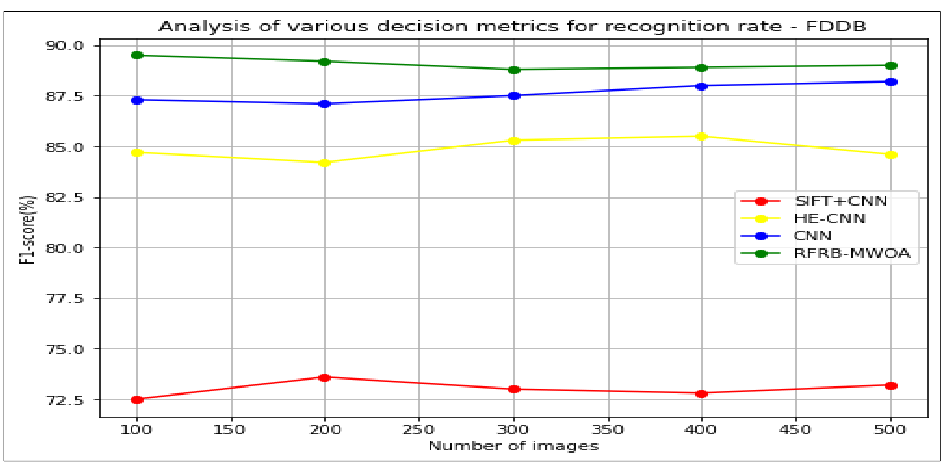

Figure 12 comparisons of F-score for FDDB dataset

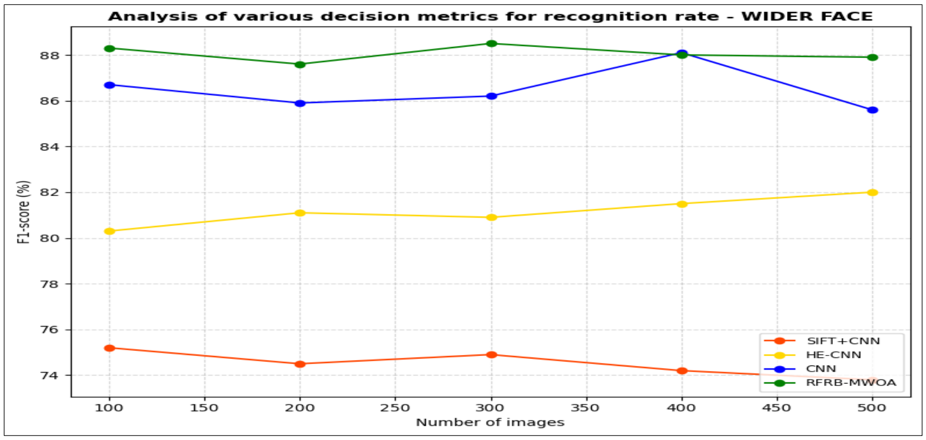

Figure 13 comparison of F-score for WIDER FACE dataset

5. Discussion

Table 1 provides a comparative analysis of various methods applied to the FDDB and WIDER FACE datasets, including SIFT+CNN [26], HE-CNN [27], CNN [21], and the proposed method, RFRB-MWOA. The evaluation is based on standard classification metrics: precision, recall, and F-score.

The comparative analysis highlights the superior performance of the proposed RFRB-MWOA method across both the FDDB and WIDER FACE datasets in terms of precision, recall, and F-score. On the FDDB dataset, RFRB-MWOA achieves the highest precision (92%), recall (93%), and F-score (89%), demonstrating its effectiveness in accurately detecting and localizing faces. Similarly, on the WIDER FACE dataset, it outperforms competing methods with precision (94%), recall (91%), and F-score (87%), showcasing its ability to balance precision and recall effectively.

In contrast, other methods, including SIFT+CNN [26], HE-CNN [27], and CNN [21], exhibit varied performance levels. For instance, SIFT+CNN shows relatively good precision on the FDDB dataset but lower recall and F-score compared to RFRB-MWOA. HE-CNN demonstrates high precision on FDDB but lags behind in recall and F-score. While CNN performs competitively on the WIDER FACE dataset, it does not surpass RFRB-MWOA on either dataset.

Overall, the results underline the notable improvements offered by RFRB-MWOA, achieving superior accuracy across all key metrics. For the FDDB dataset, RFRB-MWOA outperforms SIFT+CNN (89% precision, 86% recall, 72% F-score), HE-CNN (72% precision, 75% recall, 85% F-score), and CNN (81% precision, 89% recall, 87% F-score). Similarly, on the WIDER FACE dataset, RFRB-MWOA achieves better results than SIFT+CNN (78% precision, 74% recall, 79% F-score), HE-CNN (81% precision, 81% recall, 74% F-score), and CNN (89% precision, 86% recall, 82% F-score).

These findings emphasize the consistent superior performance of RFRB-MWOA across datasets, highlighting its ability to deliver higher accuracy in precision, recall, and F-score. However, further analysis may be warranted to explore specific advantages and limitations of each method, including computational efficiency and robustness to image quality and facial characteristic variations.

Table 1 Overall comparative analysis

FDDB dataset				**WIDER FACE dataset**		
Method	**Precision (%)**	**Recall (%)**	**F-score (%)**	**Precision (%)**	**Recall (%)**	**F-score (%)**
SIFT+CNN [26]	89	86	72	78	79	74
HE-CNN [27]	72	75	85	81	74	81
CNN [21]	81	89	87	89	82	86
RFRB-MWOA [proposed]	92	93	89	94	91	87

5.1Limitations

While mask_CNNs demonstrate proficiency in solving a wide array of problems with an elevated probability of completion, they are not without limitations and require continuous improvement. Although mask_CNNs are promising in biometric verification, expression recognition, and identifying anomalies, these applications are still in the early stages, necessitating further research to enhance accuracy and precision. Despite the considerable potential of these findings and models, they also have inherent drawbacks. For instance, authentication models can encounter difficulties verifying users in specific settings, and sensor failures can occur. Facial recognition algorithms can also struggle under particular lighting conditions, leading to erroneous facial recognition. These limitations indicate the importance of ongoing refinement and innovation in developing mask_CNNs. This will help address the challenges and maximize their effectiveness across various applications. Continued research efforts to mitigate these limitations will be essential in unlocking the full potential of mask_CNNs in biometric verification and anomaly detection.

A complete list of abbreviations is listed in *Appendix I*.

6. Conclusion and future work

The RFRB-MWOA technique offers promising answers to the occlusion and noise difficulties in face recognition applications. The method significantly enhances accuracy and robustness by using cutting-edge techniques such as Mask_CNN for feature extraction, histogram equalization for image normalization, and MWOA for hyperparameter optimization. Probabilistic max-pooling and a layered activation method serve to ensure the conservation of crucial facial traits, allowing for accurate recognition even in the presence of occlusions and distortion. Experimental results reveal that RFRB-MWOA outperforms existing approaches in many real-world scenarios. The performance of the proposed approach was evaluated using the WIDER FACE dataset, which contains 32,203 images and 393,703 annotated faces of various scales, postures, and occlusions. This dataset, which is divided into 61 event categories, serves as a comprehensive baseline for assessing the durability of face recognition systems under stressful conditions. Future study should focus on improving the system's computational efficiency for real-time applications, as well as optimizing it to handle more complex occlusions, such as severe posture shifts and partial occlusion. Furthermore, the technique might be adapted to incorporate more diverse datasets, demonstrating its usefulness in a broader range of locations and scenarios.

Acknowledgment

None.

Conflicts of interest

The authors have no conflicts of interest to declare.

Data availability

The WIDER FACE dataset utilized in this study is publicly accessible and can be found at https://www.kaggle.com/datasets/vinayakshanawad/face-mask-segmentation-wider-face-dataset and used FDDB dataset found at https://www.kaggle.com/datasets/cormacwc/fddb-dataset.

Author's contribution statement

Ms. M. Leelavathi: System model, Related work, Evaluation and analysis Conceptualization, Data collection, Writing – review and editing**. D. Kannan:** Examine and correct the manuscript, supervision, Writing – review and editing.

References

[1] Sezer OB, Dogdu E, Ozbayoglu AM. Context-aware computing, learning, and big data in internet of things: a survey. IEEE Internet of Things Journal. 2017; 5(1):1-27.

[2] De KA, Bart Y, Gu X, Liu SQ, Robinson SG, Kannan PK. Opportunities and challenges of using biometrics for business: developing a research agenda. Journal of Business Research. 2021; 136:52-62.

[3] Alwan HB, Ku-mahamud KR. Cancellable face template algorithm based on speeded-up robust features and winner-takes-all. Multimedia Tools and Applications. 2020; 79(39):28675-93.

[4] Cui K. Interacting with ubiquitous IoT devices via RF sensing. Doctorate Dissertation, Hong Kong Polytechnic University. 2023.

[5] Carlaw S. Impact on biometrics of Covid-19. Biometric Technology Today. 2020; 2020(4):8-9.

[6] Salau AO, Jain S. Feature extraction: a survey of the types, techniques, applications. In international conference on signal processing and communication 2019 (pp. 158-64). IEEE.

[7] Singh G, Chhabra I. Effective and fast face recognition system using complementary OC-LBP and HOG feature descriptors with SVM classifier. Journal of Information Technology Research. 2018; 11(1):91-110.

[8] Shi Q, Li H, Shen C. Rapid face recognition using hashing. In computer society conference on computer vision and pattern recognition 2010 (pp. 2753-60). IEEE.

[9] Seetharaman K. Image retrieval based on micro-level spatial structure features and content analysis using full range gaussian Markov random field model.

Engineering Applications of Artificial Intelligence. 2015; 40:103-16.
[10] Hatamikia S, Maghooli K, Nasrabadi AM. The emotion recognition system based on autoregressive model and sequential forward feature selection of electroencephalogram signals. Journal of Medical Signals & Sensors. 2014; 4(3):194-201.
[11] He R, Tan T, Davis L, Sun Z. Learning structured ordinal measures for video-based face recognition. Pattern Recognition. 2018; 75:4-14.
[12] Pujol FA, Pujol M, Jimeno-morenilla A, Pujol MJ. Face detection based on skin color segmentation using fuzzy entropy. Entropy. 2017; 19(1):1-22.
[13] Das A, Dantcheva A, Bremond F. Mitigating bias in gender, age and ethnicity classification: a multi-task convolution neural network approach. In proceedings of the European conference on computer vision workshops 2018 (pp. 573-85). ACM.
[14] Zhang F, Yu Y, Mao Q, Gou J, Zhan Y. Pose-robust feature learning for facial expression recognition. Frontiers of Computer Science. 2016; 10:832-44.
[15] Zafeiriou S, Zhang C, Zhang Z. A survey on face detection in the wild: past, present and future. Computer Vision and Image Understanding. 2015; 138:1-24.
[16] Tu H, Li K, Zhao Q. Robust face recognition with assistance of pose and expression normalized albedo images. In proceedings of the 5th international conference on computing and artificial intelligence 2019 (pp. 93-9). ACM.
[17] Chen X, Lan X, Liang G, Liu J, Zheng N. Pose-and-illumination-invariant face representation via a triplet-loss trained deep reconstruction model. Multimedia Tools and Applications. 2017; 76:22043-58.
[18] Ding C, Xu C, Tao D. Multi-task pose-invariant face recognition. IEEE Transactions on image Processing. 2015; 24(3):980-93.
[19] Luque J, Cortes G, Segura C, Maravilla A, Esteban J, Fabregat J. End-to-end photopleth YsmographY (PPG) based biometric authentication by using convolutional neural networks. In 26th European signal processing conference 2018 (pp. 538-42). IEEE.
[20] Donuk K, Arı A, Özdemir MF, Hanbay D. Deep feature selection for facial emotion recognition based on BPSO and SVM. Journal of Polytechnic. 2023; 26(1):131-42.
[21] Lokku G, Reddy GH, Prasad MG. OPFaceNet: optimized face recognition network for noise and occlusion affected face images using hyperparameters tuned convolutional neural network. Applied Soft Computing. 2022; 117:108365.
[22] Sahan JM, Abbas EI, Abood ZM. A facial recognition using a combination of a novel one dimension deep CNN and LDA. Materials Today: Proceedings. 2023; 80:3594-9.
[23] Febrian R, Halim BM, Christina M, Ramdhan D, Chowanda A. Facial expression recognition using bidirectional LSTM-CNN. Procedia Computer Science. 2023; 216(2022):39-47.
[24] Hu Z, Tereykovskiy I, Zorin Y, Tereykovska L, Zhibek A. Optimization of convolutional neural network structure for biometric authentication by face geometry. In advances in computer science for engineering and education 2019 (pp. 567-77). Springer International Publishing.
[25] Page A, Kulkarni A, Mohsenin T. Utilizing deep neural nets for an embedded ECG-based biometric authentication system. In biomedical circuits and systems conference 2015 (pp. 1-4). IEEE.
[26] Benradi H, Chater A, Lasfar A. A hybrid approach for face recognition using a convolutional neural network combined with feature extraction techniques. IAES International Journal of Artificial Intelligence. 2023; 12(2):627-40.
[27] Anwarul S, Choudhury T, Dahiya S. A novel hybrid ensemble convolutional neural network for face recognition by optimizing hyperparameters. Nonlinear Engineering. 2023; 12(1):20220290.
[28] Revathy G, Raj KB, Kumar A, Adibatti S, Dahiya P, Latha TM. Investigation of E-voting system using face recognition using convolutional neural network (CNN). Theoretical Computer Science. 2022; 925:61-7.
[29] Wen Y, Zhang K, Li Z, Qiao Y. A discriminative feature learning approach for deep face recognition. In computer vision–ECCV: 14th European conference, Amsterdam, the Netherlands 2016 (pp. 499-515). Springer International Publishing.
[30] Abd EM, Mirjalili S. A hyper-heuristic for improving the initial population of whale optimization algorithm. Knowledge-Based Systems. 2019; 172:42-63.
[31] Rahnamayan S, Tizhoosh HR, Salama MM. Quasi-oppositional differential evolution. In congress on evolutionary computation 2007 (pp. 2229-36). IEEE.
[32] http://shuoyang1213.me/WIDERFACE/. Accessed 20 August 2024.
[33] Jain V, Learned-miller E. FDDB: a benchmark for face detection in unconstrained settings. UMass Amherst Technical Report; 2010:1-11.
[34] Sonon SJ, Djara T, Bello AW, Ousmane M. Securing the user registration process in an IP telephony system using blockchain and KYC technologies. Journal of Scientific and Engineering Research. 2024; 11(1):238-47.
[35] Vadim S, Firdaus M, Rhee KH. Privacy-preserving decentralized biometric identity verification in car-sharing system. Journal of Multimedia Information System. 2024; 11(1):17-34.
[36] Guleria A, Krishan K, Sharma V, Kanchan T. Global adoption of facial recognition technology with special reference to India-present status and future recommendations. Medicine, Science and the Law. 2024; 64(3): 236-244.

M. Leelavathi is an Assistant Professor in the Department of AI and ML at Sree Saraswathi Thyagaraja College (Autonomous), Pollachi, and a Research Scholar at Pollachi College of Arts and Science, Pollachi. She has 10 years of experience as an Assistant Professor in various colleges. She obtained her MCA and M.Phil. (Computer Science) from Bharathiar University, Coimbatore, Tamil Nadu, India. She is currently pursuing her Ph.D. in Artificial Intelligence with a focus on Biometrics at Pollachi College of Arts and Science, Pollachi, and an MBA (Data Science and Analytics) at Manipal University. She is a Life Member of IAENG, IEDRC, and CSI. She has published seven books, filed five patents, and authored ten research articles. Her areas of research include Biometrics, Artificial Intelligence, Data Mining, Pattern Recognition, Image Processing, and Neural Networks.
Email: leelavathi.mphil86@gmail.com

Dr. D. Kannan is the Principal and a Professor of Computer Science at Pollachi College of Arts and Science, Pollachi. He obtained his Bachelor's degree in Physics from Bharathiar University, Tamil Nadu, and a Postgraduate Diploma in Computer Applications (PGDCA) from Bharathiar University. He also holds a Master's degree in Physics from Bharathiar University, a Diploma in System Analysis and Data Processing from Annamalai University, an M.Phil. in Computer Science from Bharathiar University, and an MCA from Bharathiar University, Tamil Nadu. He earned his Ph.D. in Computer Science from Bharathiar University, Tamil Nadu, India.
Email: kd.khannan@gmail.com

Appendix I

S. No.	Abbreviation	Description
1	Bi-LSTM	Bidirectional Long Short-Term Memory
2	BPSO	Binary Particle Swarm Optimization
3	CNN	Convolutional Neural Network
4	DL	Deep Learning
5	DNN	Deep Neural Network
6	ECG	Electrocardiogram
7	ELU	Exponential Linear Unit
8	FDDB	Face Detection Dataset and Benchmark
9	FLBP	Fuzzy Local Binary Pattern
10	FS-ROA	Fitness Sorted Rider Optimization Algorithm
11	GWO	Grey Wolf Optimization
12	GPSO	Graph Based Particle Swarm Optimization
13	GPU	Graphics Processing Unit
14	HE-CNN	Hybrid Ensemble Convolutional Neural Network
15	HOG	Histogram of Oriented Gradient
16	IoT	Internet of Things
17	KYC	Final Know Your Customer
18	LBP	Local Binary Pattern
19	LDP	Local Derivative Pattern
20	LFW	Labelled Faces in the Wild
21	LTD	Local Ternary Pattern
22	mask_CNN	Mask_Convolutional Neural Network
23	ML	Machine Learning
24	MWOA	Modified Whale Optimization Algorithm
25	NRLBP	Noise-Resistant Local Binary Pattern
26	OPFaceNet	Optimal Face Recognition Network
27	ReLU	Rectified Linear Unit
28	RFRB-MWOA	Robust Facial Recognition in Biometric Authentication using the Modified Whale Optimization Algorithm
29	SIFT	Scale-Invariant Feature Transform
30	SVM	Support Vector Machine
31	WLB	Weber's Local Descriptor
32	WoT	Web of Things